

Lagrangian Transport Signatures in Models and Observations

PI: A. D. Kirwan, Jr.

University of Delaware, Robinson Hall, Newark, DE 19716
phone: (302) 831-2977 fax: (302) 831-6521 email: adk@udel.edu

CO-PI: Helga S. Huntley

University of Delaware, Robinson Hall, Newark, DE 19716
phone: (302) 831-1175 fax: (302) 831-6521 email: helgah@udel.edu

CO-PI: Bruce L. Lipphardt, Jr.

University of Delaware, Robinson Hall, Newark, DE 19716
phone: (302) 831-6836 fax: (302) 831-6521 email: brucel@udel.edu

Award Number: N00014-10-1-0522

http://lagrange.ceoe.udel.edu/~helga/LOD/lagr_anal.html

LONG-TERM GOALS

We are interested in describing and understanding the processes that influence individual particle trajectories and their collective behavior, in terms of such quantities as dispersion and cohesion, and the statistics thereof. In order to achieve this goal we rely heavily on state-of-the-art, data assimilating ocean models. In spite of extensive Eulerian validation, the reliability of the models' Lagrangian forecasts remains uncertain. Thus, we strive to rectify this situation by analyzing the correspondence of modeled features with available observations. The insights gained from such a study should inform both interpretation of model results and model development.

OBJECTIVES

The main objectives of this effort are to identify the signatures of ocean transport processes in both observations and models and to assess the uncertainty in these model predictions. Scientifically, our interest is in the ocean dynamics responsible for mesoscale features and their interaction with flows at other scales. Our primary concern is the evolution of eddies and the development of fronts near strong jets, in both models and observations. In FY10, our focus was predominantly on developing methods for defining, locating, and tracking eddy centers and boundaries, with an initial foray into the analysis of the water mass exchange between eddies and their environment.

APPROACH

The first step for a study of the interaction of eddies with their environment is to identify the eddies. This is, in fact, a more complex task than it appears at first glance, as there is no generally accepted consensus of what defines an eddy. Beyond the broad agreement that it involves vortical flow, there have been various suggestions falling into two main categories, with some methods straddling both

groups: those based on the geometry of the velocity field and those based on the physical properties of the flow field (e.g. vorticity, sea surface height, Okubo-Weiss parameter). Proposed definitions are typically tested against the “you know it when you see it” standard. This is scientifically unsatisfactory but for the time being remains the only option, since no method so far has managed a 100% success of detection rate with a 0% excess detection error.

We have chosen to implement the geometry-based eddy detection algorithm proposed by *Nencioli et al., 2010* (hereafter “N10 algorithm”). A location in a velocity field is deemed an eddy center if it passes four tests:

1. The north-south velocity v changes sign along an east-west section through the eddy and its magnitude increases away from the center;
2. the east-west velocity u changes sign along a north-south section through the eddy and its magnitude increases away from the center;
3. the eddy center is a local minimum in the velocity magnitude field; and
4. the sense of rotation around the eddy center is consistent without excessive jumps (i.e. velocity vectors at neighboring grid points along a square around the center must have complex angles within 90° of each other).

The numerical algorithm can be tuned to detect eddies of a minimum size and with a minimum separation distance. We have reduced these two parameters to a single length scale representing a typical minimum diameter of the eddies we want to detect.

This automatic eddy detection scheme was applied to model velocity fields from two Gulf of Mexico (GoM) models. A single time slice from each model was used to determine an error rate (failure to detect and excess detection). Subsequently, a time series of eddy counts across the entire GoM basin with error bars was generated for a two-month period for each model.

The two models chosen are CUPOM with a resolution of $1/12^\circ$ and GOM-HYCOM with a resolution of about $1/25^\circ$. In each case, we focused on the surface layer. The statistics of the two time series permit an estimation of mesoscale activity in the GoM. A comparison between them gives an indication of the role of model grid resolution, even though the models do not cover the same time period. In the future, we also intend to move further down into the water column to investigate the three-dimensional nature of these eddies.

Once an eddy center is identified, it remains to determine its extent. This is an even more challenging task, since the “you know it when you see it” test yields uncertain results. Each physical property-based definition of an eddy is associated with a boundary criterion, characterized by a somewhat arbitrarily chosen cut-off value. Geometry-based approaches sometimes also result in a natural boundary criterion, as for example for the definition using instantaneous streamlines (*Chaigneau et al., 2008*). *Nencioli et al., 2010*, suggests a method based on an approximate streamfunction.

Side-stepping some of the issues associated with locating eddy centers, we have focused on one clearly identifiable eddy, namely the Loop Current ring Fourchon in the GoM in April 1998. The center was defined as an instantaneous stagnation point inside the vortex. Several different boundary algorithms were then tested:

1. first inflection point in the speed along outward radials (local maxima), with or without an imposed minimum value;
2. the mean of the largest spiraling instantaneous streamlines started on radials at 1° intervals subject to a maximum endpoint separation and a maximum change in area from that contained in the next smaller streamline;
3. the largest closed sea surface height (SSH) contour with a minimum value; and
4. the outermost closed approximate streamfunction contour across which velocity magnitudes are still increasing (checked only in the four main directions aligned with the grid) as in *Nencioli et al., 2010*.

Methods 2 and 3 yielded the most satisfactory and often very similar results, but method 3 is significantly faster computationally. It was hence chosen to begin an investigation into the fluid mass exchange of Fourchon with its surrounding waters by tracking the Eulerian evolution along with the Lagrangian evolution of the eddy boundary.

WORK COMPLETED

In FY10, we focused our effort on the identification and tracking of eddies. Specifically, we

- implemented the method for locating eddy centers described in *Nencioli et al., 2010*, to compare to a simplistic elliptic instantaneous stagnation point method;
- created a preliminary error estimate of the detection algorithm based on two individual velocity fields drawn from CUPOM and GOM-HYCOM;
- generated a two-month time series of eddy counts within the basin of the GoM;
- implemented four different methods for determining eddy boundaries and tested them on two months of CUPOM velocity data for the Loop Current ring Fourchon;
- investigated the fluid exchange between Fourchon and its environment via a comparison of Lagrangian and Eulerian evolutions of the boundary;
- began collecting satellite imagery with well defined mesoscale features, in SST and chlorophyll; and
- assembled drifter observations from the GoM collected by various groups in connection with the Deepwater Horizon oil spill in the spring of 2010.

RESULTS

A simple method for finding potential eddy centers is to locate elliptic instantaneous stagnation points (ISPs) in the model velocity field. Hardly any “true” eddy centers are missed, but there is a great excess of detection, as ellipticity based on the value of the velocity Jacobian is not unique to vortical features. Moreover, ISPs often appear in stagnation curves, at least in model data, which have to be collapsed. This can be achieved through steps 3 and 4 of the N10 algorithm.

In our two test cases, the outcome of this ISP-based method was found to be very similar to that from the complete N10 algorithm, with a slightly smaller miss rate (33.9% vs. 37.5%) and a slightly higher over-prediction rate (12.5% vs. 8.9%) for a sample of 56 eddies combined for both cases. Note that

when taken separately, both error rates are significantly lower for CUPOM than for GOM-HYCOM, as shown in Table 1. We hypothesize that this is due to the greater smoothness of the CUPOM velocity field.

Table 1: Error rates for the two eddy center detection schemes applied to the two GoM models

	Miss Rate	Over-prediction Rate	Total # of “True” Eddies
CUPOM: ISP	25.0%	5.0%	20
CUPOM: N10	30.0%	5.0%	20
GOM-HYCOM: ISP	38.9%	16.7%	36
GOM-HYCOM: N10	41.7%	11.1%	36

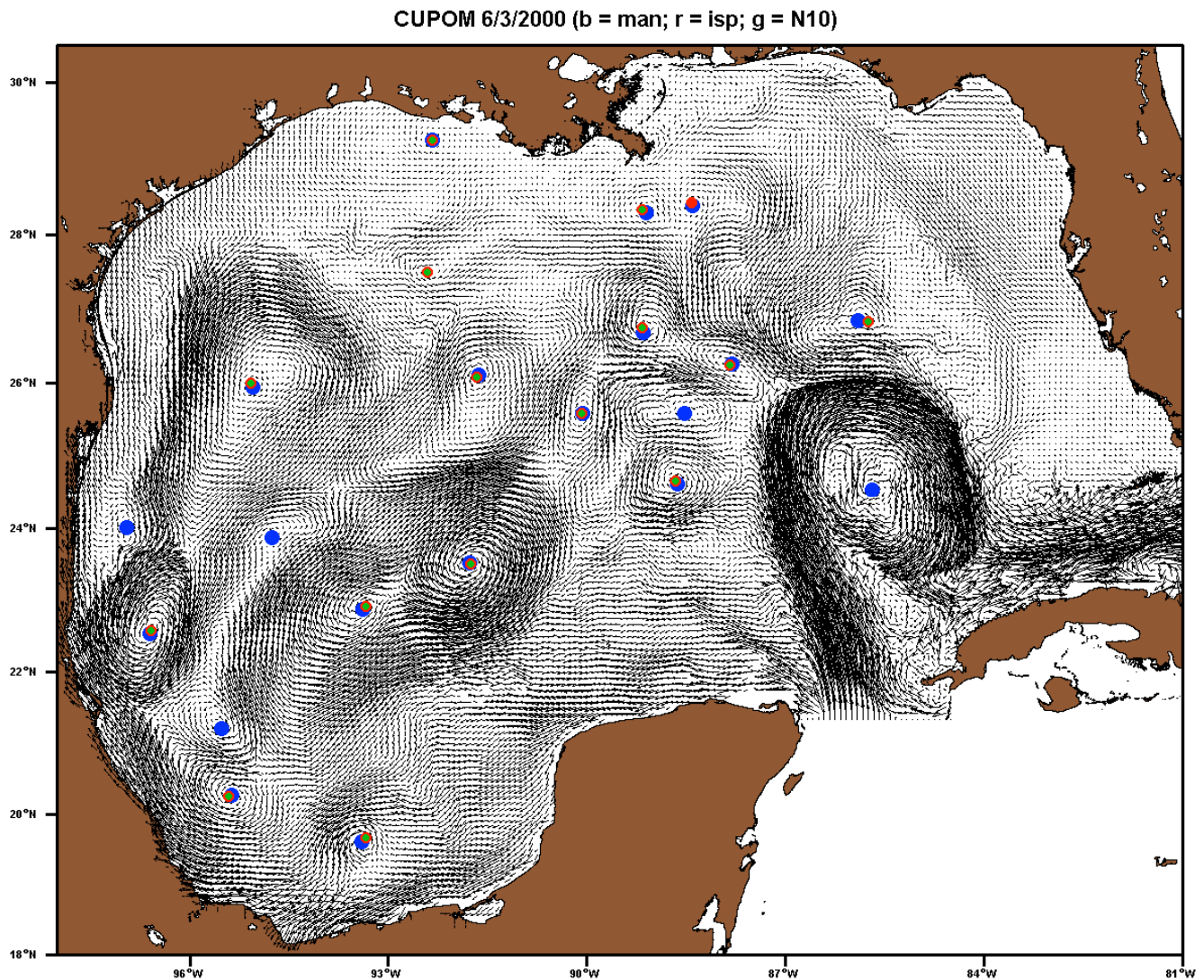


Figure 1: CUPOM surface velocity field for 3 June 2000. Manually determined eddy centers are marked in blue, those from the ISP-based algorithm in red, and those from the N10 algorithm in green. Neither of the algorithms find the almost detached Loop Current ring. They also miss several smaller eddies. There is only one location misidentified as an eddy center by both algorithms.

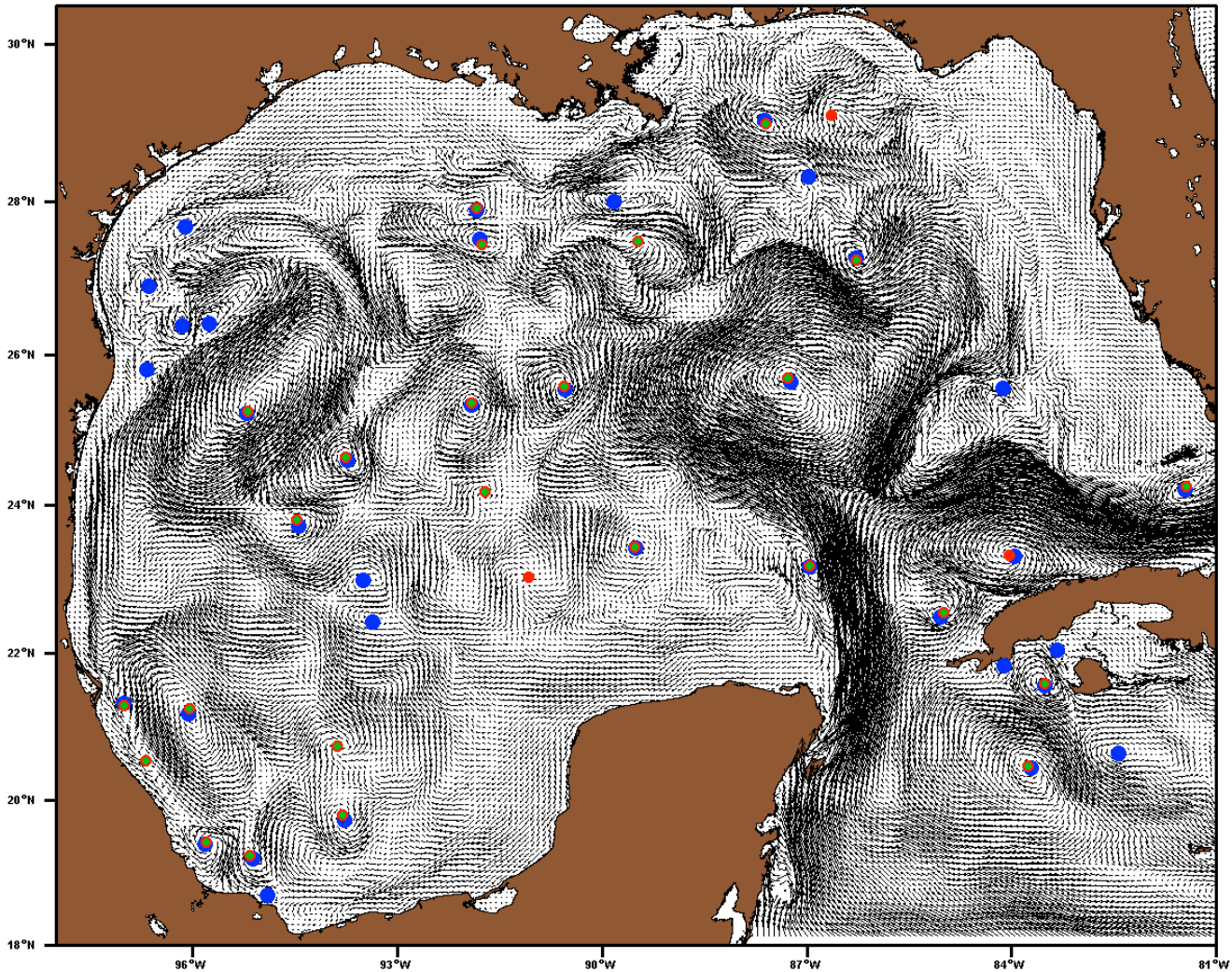


Figure 2: GOM-HYCOM surface velocity field for 27 May 2010. Manually determined eddy centers are marked in blue, those from the ISP-based algorithm in red, and those from the N10 algorithm in green. The algorithms miss several smaller eddies and misidentify spiraling flow structures as eddies. The flow field generally exhibits more mesoscale activity than the CUPOM field in Figure 1.

Figures 1 and 2 show sample velocity fields from the two models, along with the eddy center locations as identified manually and by each of the two algorithms. Examination of the problem eddy centers reveals that erroneously identified locations are primarily associated with spiraling flow. Missed locations are mainly small eddies that were likely discarded because of the chosen length scale of 50 km. One notable exception is the Loop Current ring in CUPOM, which was not detected by either algorithm. The interior of this ring is not well organized into a clear vortex, so that the local geometric criteria on the vector field fail. A thorough investigation of the impact of the chosen length scale parameter on the success and excess of detection is currently underway.

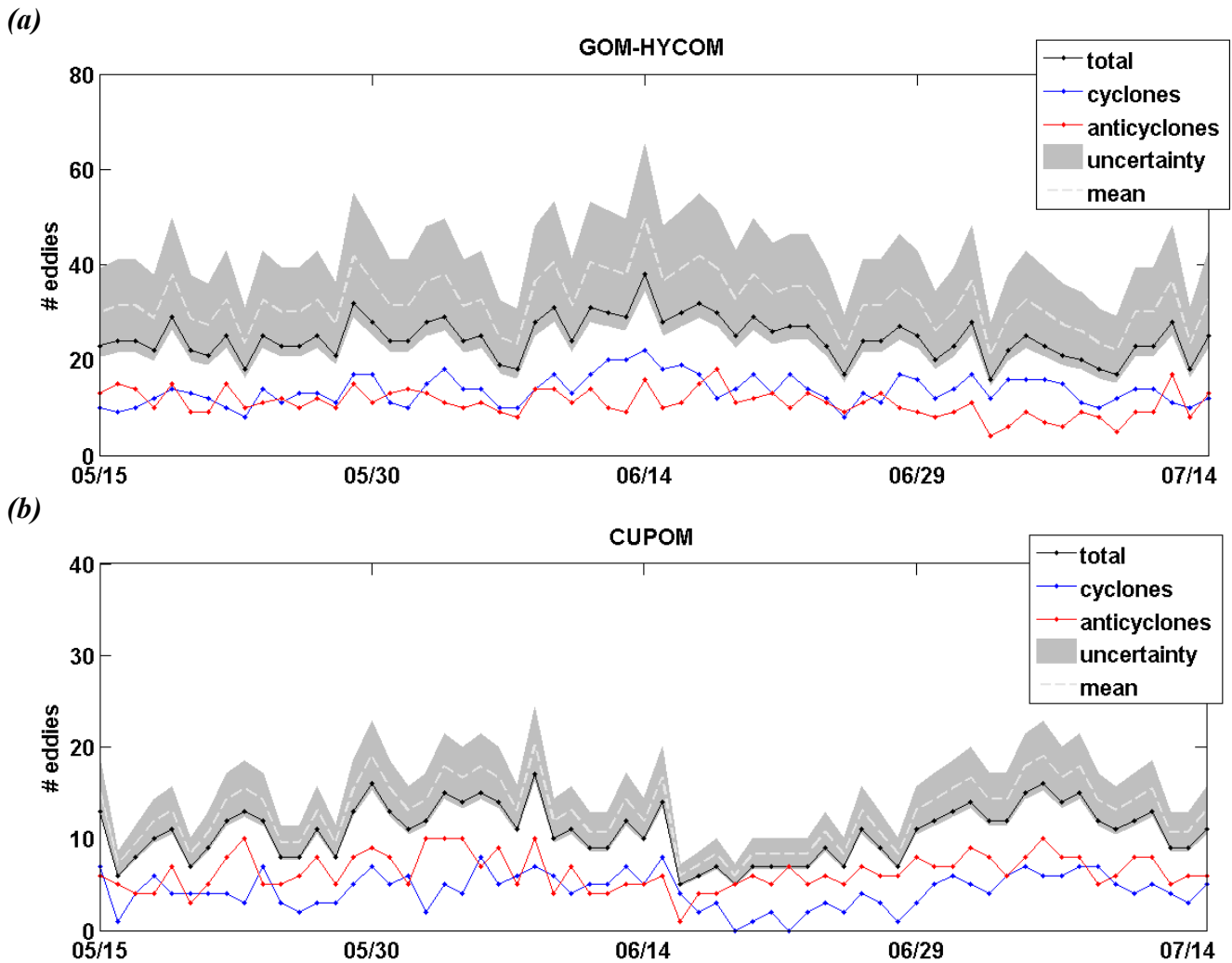


Figure 3: Time series of eddy counts in the GoM from (a) GOM-HYCOM for 15 May – 15 July 2010 and (b) CUPOM for 15 May – 15 July 2000. Total counts are marked in black, cyclones in blue, and anticyclones in red. The grey band indicates the uncertainty in the total count, with a light grey dashed line for its mean. Counts for CUPOM are about half of what they are in GOM-HYCOM. Variability overall is low. Cyclones and anticyclones appear in comparable numbers in both models.

Given the comparable performance of the two algorithms, we have chosen to focus on the N10 algorithm for creating the time series of eddy counts, because it is computationally somewhat faster. Figure 3 displays the time series for counts of all eddies (black), cyclones (blue), and anticyclones (red) over the entire GoM basin as modeled by GOM-HYCOM for 15 May 2010 until 15 July 2010 and by CUPOM for 15 May 2000 until 15 July 2000. A grey band is also plotted to indicate the uncertainty in the total eddy count, using the error rates from Table 1. The light grey dashed line shows the mean value in this uncertainty band.

The plot for GOM-HYCOM reveals that the number of eddies is remarkably constant over time; i.e., the decay rate is approximately equal to the birth rate. Moreover, while more often the number of

cyclones outnumbered that of anticyclones, the differences are fairly small: The mean number of cyclones counted over the 62 days is 14; the mean number of anticyclones is 11.

Note that the uncertainty in the eddy count is not centered on the algorithm output. From the error estimates in Table 1, we see that the undercount is much greater than the over-count. Consequently, the best estimate of the total number of eddies may well be somewhat higher than what N10 returns. Correcting for this uncertainty, the average best estimate total eddy count is 32 eddies, with a range from 21 to 50 eddies.

The situation is a bit different in the CUPOM model. The counts are generally lower, probably a result of a smoother velocity field at the lower resolution: The average best estimate total eddy count is 13, with a range from 6 to 20 eddies. The uncertainty band is significantly narrower, and the relative variability somewhat greater. Here the number of anticyclones is more often greater than that of cyclones, with again small differences (means of 6 and 4, respectively, for anticyclones and cyclones).

Which of these two characterizations of the GoM is more accurate – whether the increased eddy activity apparent in the higher resolution GOM-HYCOM reflects real small-scale features – is one of the questions we plan to investigate in the coming year through comparisons with observations. For this purpose, we have begun collecting relevant satellite imagery as well as drifter data.

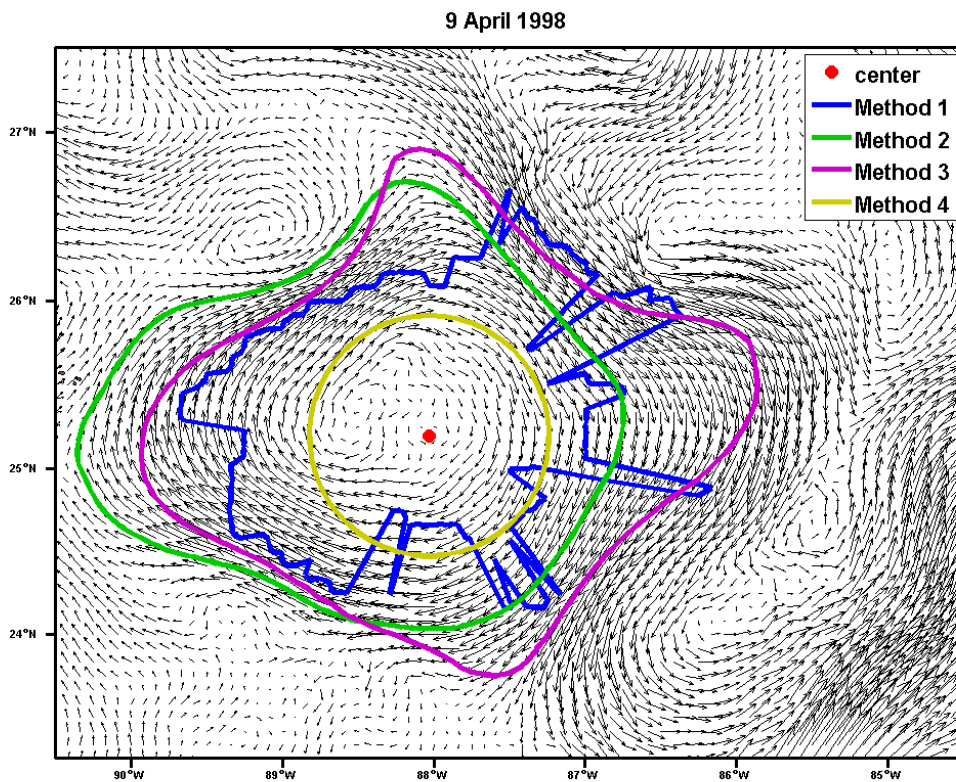


Figure 4: Loop Current ring Fourchon on 9 April 1998 as shown in the CUPOM velocity field with possible boundaries as determined by the four methods discussed in the text. Methods 2 (instantaneous streamlines) and 3 (SSH contours) produce reasonable results, while Method 1's (speed inflection) outline is too ragged and Method 4 (approximate streamfunction) defaults to a circle.

To study individual eddies and their evolution, it is important to determine not just their centers but also their boundaries. Figure 4 shows one example testing the four different methods described above. Using the speed inflection point results in a very irregular boundary. This is a typical problem for large rings like Fourchon. It also leads to Method 4 failing and defaulting to a circle with a predetermined radius: The very interior of the eddy is too messy to result in clean speed increases along radials. Both of the other methods give acceptable boundaries. In the instance shown in Figure 4, they differ noticeably, which is not always the case. Which one of the boundaries is closer to the “actual” boundary is subjective. As mentioned above, Method 3 has the advantage of computational speed, which leads us to prefer it to the others.

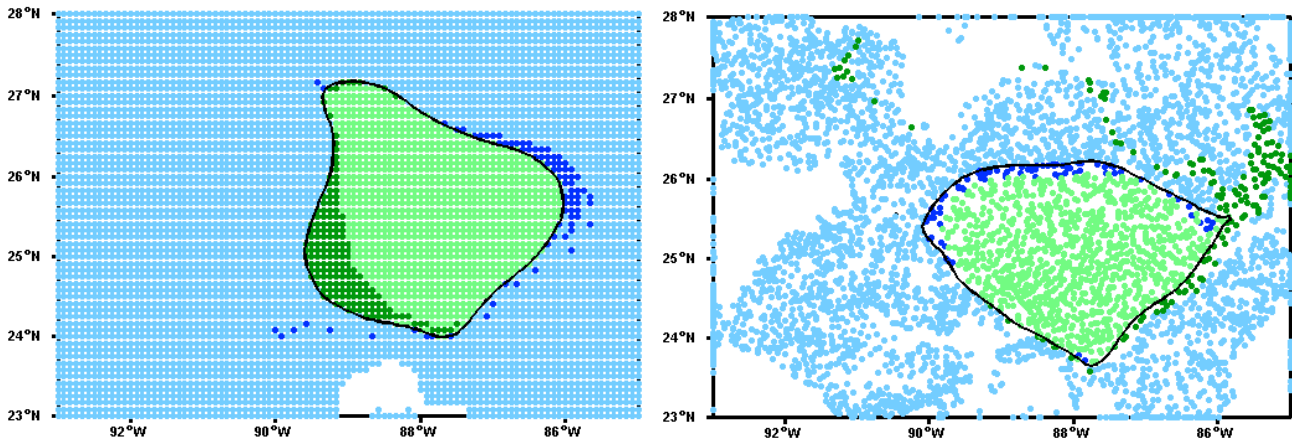


Figure 5: The evolution of Fourchon from 4 April 1998 (left) until 14 April 1998 (right). Particles launched inside the eddy on 4 April are colored in green, those launched outside in blue. The darker shade of each color denotes particles that cross the eddy boundary. There is substantial fluid exchange between the eddy and its environment. Entrainment (dark blue) in this case is predominantly local, with fluid particles from near the boundary crossing to the inside. Detrainment (dark green), on the other hand, sees particles from the inside of the eddy transported quite some distance away from the eddy.

Eddies are often thought of as masses of water in solid-body rotation. Indications that this is far too simplified a view and that the exchange between eddies and their environment plays a crucial role were reported in *Lipphardt et al., 2008*. Here we discuss early results from an investigation into this phenomenon. Figure 5 shows one example of Fourchon interacting with its surrounding environment, including fluid exchange over ten days (4 April – 14 April 1998). The boundaries in each panel are defined as closed SSH contours, an Eulerian snapshot. The Lagrangian evolution is captured in the color scheme: Green particles are launched inside the eddy on the starting date, while blue particles are launched on the outside. Particles remaining on the same side of the boundary ten days later are colored in a lighter shade. The left panel shows the uniform grid on which the particles were launched, while the right panel maps their final positions.

This example supports the idea that the fluid exchange between the ring and the surrounding water masses is, in fact, substantial. Moreover, while predominantly particles near the boundary are involved, it is immediately clear that even within the relatively short time of ten days some of the

interior particles have traveled far outside the eddy (dark green dots). We are investigating the processes responsible for this exchange. Preliminary analyses suggest that fluid is detrained from the eddy at nearby hyperbolic points, which hasten the dispersal. Over longer time periods, it is not uncommon for fluid from the eddy interior to reach the Loop Current itself and be swept out of the GoM entirely. Entrainment, on the other hand, seems to result frequently from spiraling transport patterns, which have a more localized effect.

IMPACT/APPLICATIONS

Ocean models are often used for transport predictions. Without a good estimate of the uncertainty associated with their forecasts, it is difficult to interpret the output in a practical situation. This became very obvious during the oil spill mitigation efforts in the GoM after the explosion of the Deepwater Horizon drilling platform earlier this year. It is often assumed that the accuracy of ocean models is limited primarily by bounds on the resolution due to finite computational resources. Higher resolution models do produce more smaller scale features in the flow field. However, it remains unclear whether these improve or degrade transport forecasts based on model output. This funded effort will provide insight into this problem. The work reported here lays the foundation by developing methods for describing the model oceans, specifically their eddy activity.

RELATED PROJECTS

This project is closely related to three other ONR projects by the same principal investigators:

N00014-11-1-0087: Dynamical systems theory in 4D geophysical fluid dynamics – This newly funded MURI program is concerned with moving Lagrangian analysis of general circulation models from two (horizontal) spatial dimensions to three full dimensions. While currently most calculations are restricted to individual layers of a model, this work will connect these and develop methods for understanding the 3D evolution of Lagrangian coherent structures.

N00014-09-1-0703: How well do blended velocity fields improve the predictions of drifting sensor tracks? – For this effort, we collaborated with colleagues at RSMAS, University of Miami, to investigate two different methods of data blending and their effectiveness for improving trajectory forecasts. We have found that assimilating drifter observations can yield great improvements in independent sonobuoy drift predictions (*Chang et al., 2010*).

N00014-09-1-0559: Assessing the Lagrangian predictive ability of Navy ocean models – This work aims to estimate uncertainty in ocean models by analyzing ensembles of model runs from operational Navy models.

N00173-08-1-G009: Prediction of evolving acoustic sensor arrays – This effort is focused on demonstrating how Lagrangian analysis of Navy ocean model predictions can be performed at a Navy operational center and how Lagrangian products can be delivered to fleet operators on scene in near-real time to support tactical decision making.

N00014-07-1-0730: Enhanced ocean predictability through optimal observing strategies – For this project, we applied synoptic Lagrangian tools to a regional ocean model off the coast of northern

California as a proof of concept exercise demonstrating how knowledge of the evolving ocean might aid fleet operators concerned with optimizing AUV deployments in the coastal ocean.

REFERENCES

Chaigneau, Alexis, Arnaud Gizolme, and Carmen Grados, Mesoscale eddies off Peru in altimeter records: Identification algorithms and eddy spatio-temporal patterns, *Prog. Oceanogr.*, 79 (2-4), 106-119, 2008.

Chang, Y., D. Hammond, A. C. Haza, P. Hogan, H. S. Huntley, A. D. Kirwan, Jr., B. L. Lipphardt, Jr., V. Taillandier, A. Griffa, T. M. Özgökmen, Enhanced estimation of sonobuoy trajectories by velocity reconstruction with near-surface drifters, *Ocean Model.*, submitted and revised, 2010.

Lipphardt, B. L., Jr., A. Poje, A. D. Kirwan, Jr., L. Kantha, and M. Zweng, Death of three Loop Current rings, *J. Mar. Res.* 66, 25-60, 2008.

Nencioli, Francesco, Changming Dong, Tommy Dickey, Libe Washburn, and James C. McWilliams, A vector geometry-based eddy detection algorithm and its application to a high-resolution numerical model product and high-frequency Radar surface velocities in the Southern California Bight, *Journal of Atmospheric and Oceanic Technology*, 27(3), 564-579, 2010.

PUBLICATIONS

Auladell, M., J. L. Pelegrí, A. García-Olivares, A. D. Kirwan Jr., B. L. Lipphardt Jr., J. M. Martín, A. Pascual, P. Sangrà, M. Zweng, Modelling the early evolution of a Loop Current ring, *J. Mar. Syst.*, 80, 160-171, 2010 [published, refereed].

Branicki, M and A. D. Kirwan, Jr., Stirring, the Eckart paradigm revisited, *Int. J. Engr. Sci.*, 2010 [in press, refereed].

Chang, Y., D. Hammond, A. C. Haza, P. Hogan, H. S. Huntley, A. D. Kirwan, Jr., B. L. Lipphardt, Jr., V. Taillandier, A. Griffa, and T. M. Özgökmen, Enhanced estimation of sonobuoy trajectories by velocity reconstruction with near-surface drifters, *Ocean Model.*, 2010 [submitted, refereed].

Huntley, H. S., B. L. Lipphardt, Jr., and A. D. Kirwan Jr., Lagrangian predictability assessed in the East Asia Sea, *Ocean Model.*, 2010 [submitted, refereed].